

MULTIPLE DEGREE-OF-FREEDOM FORCE AND MOMENT MEASUREMENT  
 FOR STATIC PROPULSION TESTING USING  
 MAGNETIC SUSPENSION TECHNOLOGY

512-14  
 163492

By  
 Keith Stuart  
 Blake Bartosh  
 Innovative Information Systems  
 an Aura Systems Company

P-14

## 1.0 INTRODUCTION

Innovative Information Systems (IIS), Inc. is in the process of designing and fabricating a high bandwidth Force and Moment Measuring device (i.e. the Magnetic Thruster Test Stand). This device will use active magnetic suspension to allow direct measurements of the forces and torques generated by the rocket engines of the missile under test. (See figures 1-1, 2-1, 2-2, 3-1 through 3-4, and 4-1 through 4.8.)

The principle of operation of the Magnetic Thruster Test Stand (MTTS) is based on the ability to perform very precise, high bandwidth force and position measurements on an object suspended in a magnetic field. This ability exists due to the fact that the digital servo control mechanism that performs the magnetic suspension uses high bandwidth (10 kHz) position data (via an eddy-current proximity sensor) to determine the amount of force required to maintain stable suspension at a particular point. This force is converted into required electromagnet coil current, which is then output to a current amplifier driving the coils. Figure 1-1 shows a conceptual diagram of the MTTS system components.

Section 2 contains a discussion of how the coil current and magnetic gap distance (the distance between the electromagnet and the object being suspended) is used to determine the forces being applied from the suspended assembly. If the suspended object contains a firing rocket thruster, the force of the thruster will create a motion that tends to drive the suspended object towards the opposite electromagnets. The proximity sensors will sense this motion, and the digital processor will command coil currents thus creating the servo force necessary to cancel the thruster force. The suspension servo will have the ability to cancel any forces that occur within the servo's closed loop bandwidth.

Any forces having frequency components above the servo bandwidth will cause the suspended assembly to accelerate. The motion caused by this acceleration will be tracked by the proximity sensors, and the acceleration will also be measured directly with accelerometers. Multiplying the acceleration with the suspended assembly's mass yields the force required to cause that motion. Summing the coil force with the acceleration force provides the required 10 kHz force data measurements for each pole assembly. The ability to measure high bandwidth forces well above the servo bandwidth has been demonstrated by the proof-of-concept demo, described in section 3. A 1,000 Hz sinusoidal motion disturbance was injected into a magnetically gimballed E-O seeker assembly, and measured accurately by the data acquisition and analysis system. Refer to figure 3-4.

PRECEDING PAGE BLANK NOT FILMED

182  
 INTERNATIONALLY RECOGNIZED

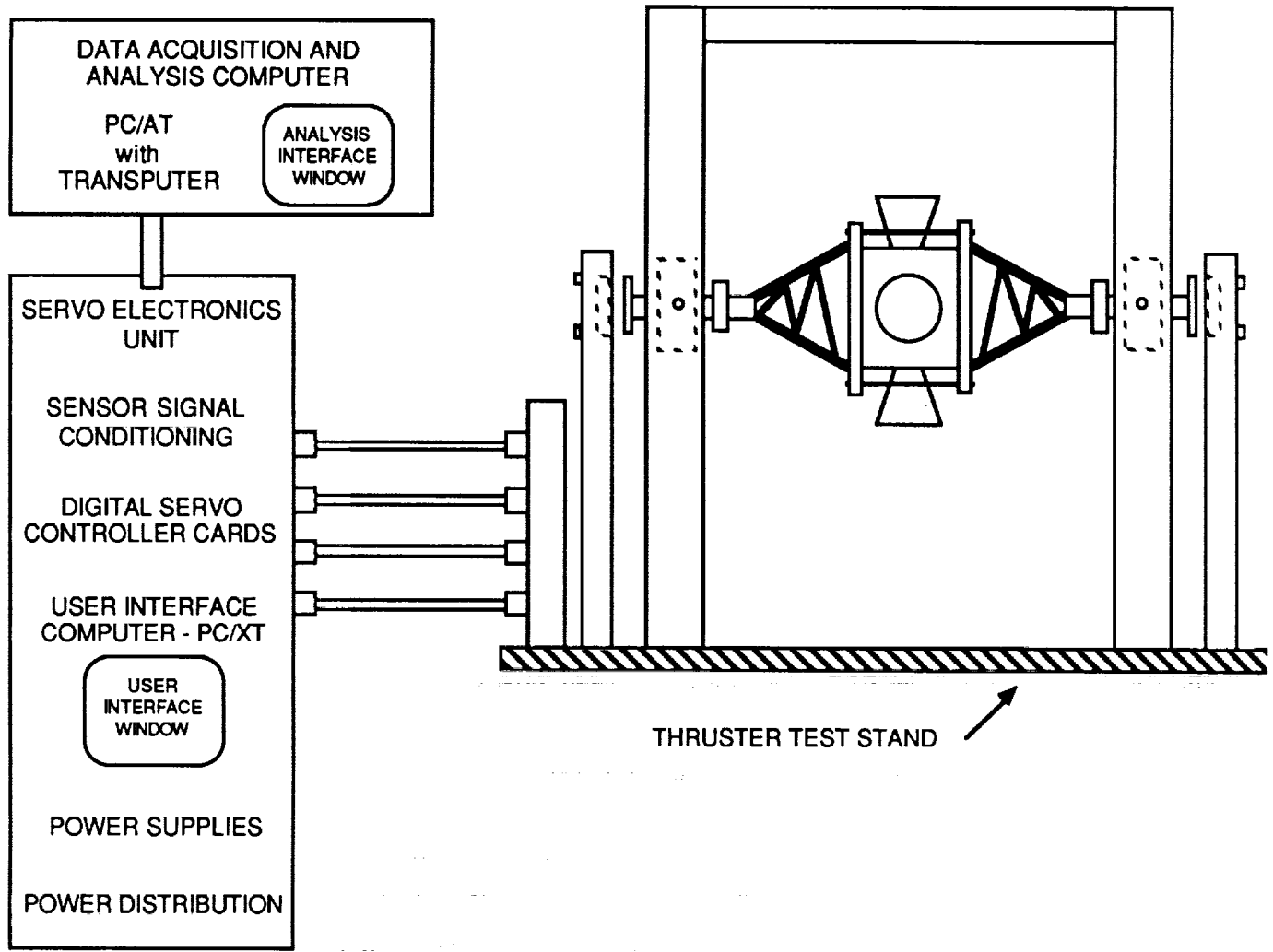


**FIGURE 1-1: MTTS SYSTEM COMPONENTS**

Individual coil forces can be summed in each of the lateral directions to provide 3 lateral force components, and differenced to provide the 3 angular torque components. Section 2 also contains a detailed discussion of the equations involved in this process.

It should be noted that the current and proximity sensor measurements taken by the data acquisition system reflect actual system conditions, not estimates of system conditions provided by the digital servo controller. The proximity sensor measurement reflects the actual gap distance, providing motion information up to its 10 kHz bandwidth. The current through the coils is measured by tracking the voltage across a resistor in series with the electromagnet coil. The digital processor is commanding that current level in discrete steps every 250 microseconds, but the actual system parameter of electromagnet coil current is the quantity that affects servo behavior, not the commanded level. By measuring the current directly, a much more accurate, higher bandwidth state of the system is obtained than would be possible if digital servo parameters were acquired.

## SECTION 2: COMPUTING ELECTROMAGNETIC FORCE

Figure 1-1 showed a conceptual diagram of the MTTS system. The two radial magnetic bearings control the radial position of the vehicle in the support assembly, the axial electromagnets control axial position, and the two rotary actuators control the pitch angle.

When a divert thruster is fired, the vehicle/support assembly will be driven towards the radial electromagnets opposite to the firing thruster. The electromagnets opposite the direction of thrust will be activated by the servo, cancelling out the force of the thruster.

The amount of force being applied by the electromagnets during the thrust is dependent on the reluctance of the magnetic circuit, the number of turns in the electromagnetic coil and the current flowing through the coil.

Figure 2-1 contains a diagram of the closed magnetic "circuit" that is used for each of the pole assemblies. The magnetic circuit is analogous to an electric circuit. The material used in the pole pieces conducts magnetic flux, as wire conducts electrical current.

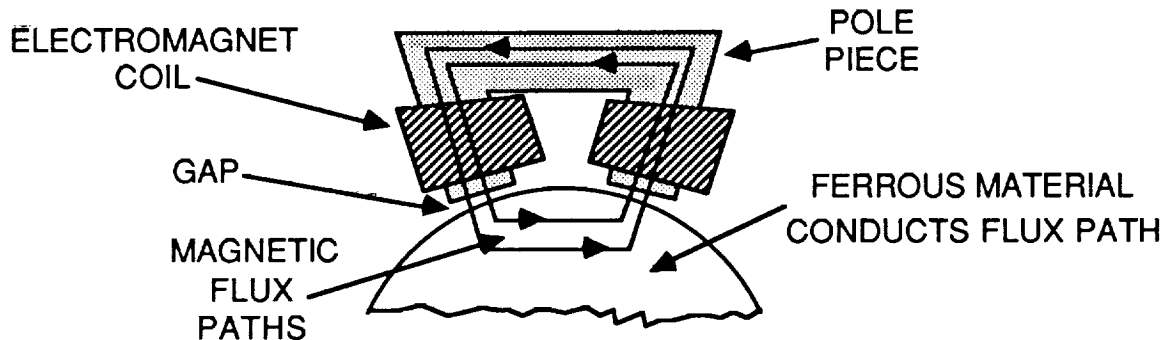


FIGURE 2-1: CLOSED MAGNETIC CIRCUIT

The reluctance of the pole assembly circuit in Figure 1-1 is computed as follows:

$$R_t = 2R_g + R_m$$

where:  $R_t$  is the total reluctance

$R_g$  is the gap reluctance

$R_m$  is the magnetic material reluctance

The reluctance of the material is a constant value that is measured during assembly. The reluctance of the magnetic gap is computed as follows:

$$R_g = \frac{l_g}{\mu_0 A_g}$$

where:  $A_g$  is the cross sectional area of the gap

$l_g$  is the gap length

$\mu_0$  is the permeability of free space

The magnetic flux density can now be computed:

$$B = \frac{N_i}{A_g R_t}$$

where:  $B$  is the magnetic flux density

$N_i$  is the number of ampere-turns

With the flux density, the force that the electromagnet is applying to the rotor is computed:

$$F_c = \frac{B^2 A_g}{\mu_0} L_f$$

where  $L_f$  is the magnetic leakage factor

The data acquisition system will update the coil current and gap width measurements every 100 microseconds.

## 2.1 Computing Force of Motion

The electromagnetic coil can only respond and cancel forces whose frequencies are below the 200 Hz closed loop servo bandwidth. Any force components above that frequency will cause a force imbalance, which will in turn cause accelerations and thus motions to the vehicle and support assemblies.

The eddy current proximity sensors possess a bandwidth of 10 kHz, and therefore can track that residual motion. Figures 4-1 through 4-6 show examples of the various time waveforms during a thrust. In that example, when the thruster is activated, the leading edge, high bandwidth component of the force will move the vehicle approximately 0.015 inches in about 5 msec until enough current has built up in the coil to balance the force and stop the motion. Accelerometers mounted on the suspended structure provide the acceleration levels. Multiplying the acceleration by the mass yields the high bandwidth force component that was not controlled by the servo.

Summing the electromagnet force computed above with the high bandwidth motion force yields a high bandwidth measurement of the force induced by the thruster.

## 2.2 Computing Total Thruster Forces and Torques

The above sections showed how high bandwidth force data was derived for an individual pole assembly. Figure 2-2 illustrates how the thruster force is distributed throughout the radial and axial poles of the system. By summing the force components of each pole assembly, the total force in the three lateral directions can be found as follows:

$$F_{x_t} = F_{x_1} + F_{x_2}$$

$$F_{y_t} = F_{y_1} + F_{y_2}$$

$$F_{z_t} = F_{z_1} + F_{z_2}$$

$F_{x_1}$ ,  $F_{y_1}$  and  $F_{z_1}$  are the force vector components at bearing 1

$F_{x_2}$ ,  $F_{y_2}$  and  $F_{z_2}$  are the force vector components at bearing 2

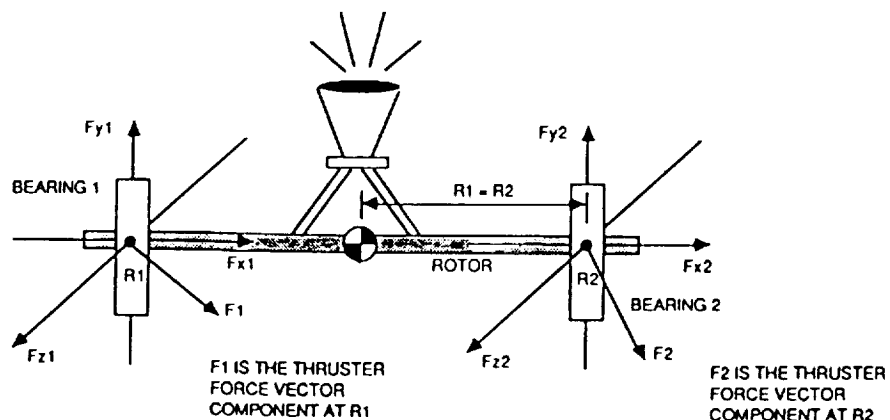


**FIGURE 2-2: THRUSTER FORCE DISTRIBUTION**

Similarly, the torques in the three angular directions can be found as follows:

$$T_{yaw} = (F_{z_1} - F_{z_2}) \times R$$

$$T_{roll} = (F_{y_1} - F_{y_2}) \times R$$

$$T_{pitch} = I_{act} \times K_{act}$$

where  $R$  is the moment arm

$I_{act}$  is the current through the rotary actuator

$K_{act}$  is the rotary actuator torque constant

Note that the torque in the pitch axis is measured directly from the angular actuator current.

### 3.0 Proof of Concept Feasibility Demo

In October, 1987, IIS modified the single axis magnetic gimbal hardware to demonstrate the feasibility of the MTS engineering approach. The following paragraphs contain a description of the hardware and the results of the testing.

Figure 3-1 contains a diagram of the hardware configuration. The basic gimbaling system consists of a pair of magnetic bearings which support a 16.5 pound structural model of a missile IR sensor mounted on an aluminum shaft. The axial direction is controlled passively by opposing Samarium Cobalt magnets on each end. The pitch angle is controlled by a rotary actuator.

The servo electronics consist of a single Motorola 68020 processor servicing the four radial suspension servos and the single rotary servo. This board is housed in a PC/AT computer, providing 5 channels of 12 bit A/D and D/A conversion.

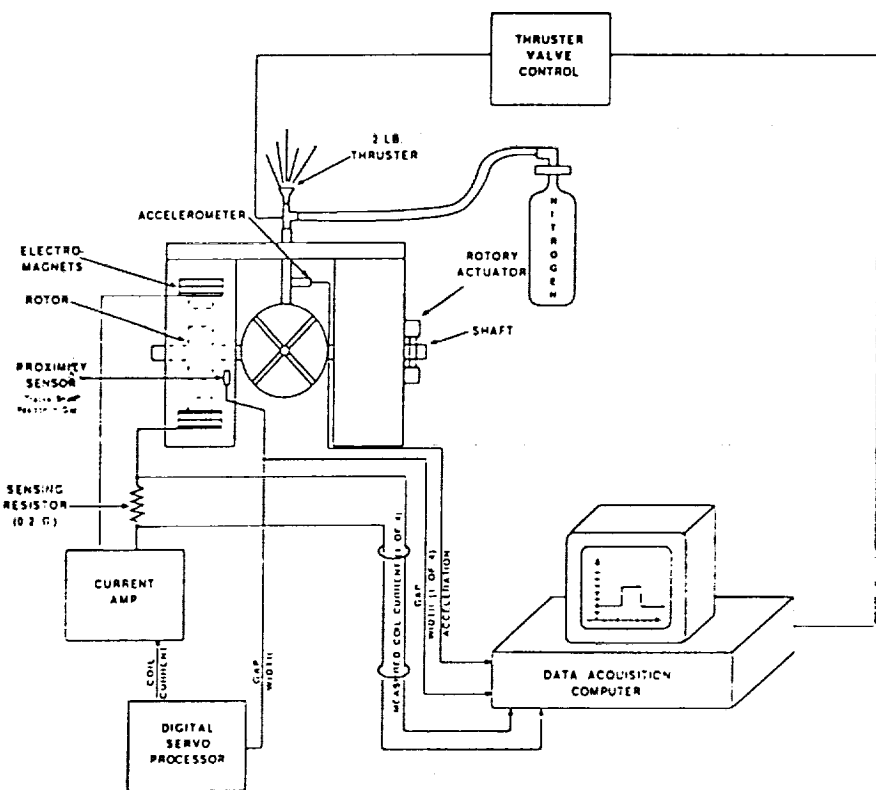


FIGURE 3-1: THRUST STAND FEASIBILITY DEMO SET-UP

A thruster support pedestal was designed and fabricated for the seeker, providing an attachment point for a 1.5 pound cold gas thruster. The thruster, associated valve driver electronics and high pressure nitrogen source was provided by Rocketdyne.

IIS constructed a rack-mounted electronic interface module providing the means to pick-off the appropriate servo signals for data acquisition. These signals were conditioned through an op-amp network, and included the following parameters:

- 4 channels of coil current data
- 4 channels of proximity sensor data
- 1 channel of accelerometer data

An 8-channel A/D converter printed circuit board was placed into the data acquisition computer (another PC/AT). To allow data acquisition of the accelerometer data, a multiplexing circuit was added to a channel of coil current data.

An additional electronic circuit was constructed to provide the means for the computer to command the thruster control valve on and off for user-defined intervals. The actual valve driver electronics was provided by Rocketdyne, commanding the high speed solenoid in the Moog thruster valve.

The software required to fire the thruster and acquire and process the data consists of 1,000 lines of assembly code to control the A/D card, 2,500 lines of "C" to un-interleave the A/D data that was dumped into computer RAM, and 3,000 lines of Fortran code to convert the raw data to engineering units and plot the results.

The fabrication of the mechanical interface, the electronic interface module and the development and debug of the software was accomplished in 3 weeks.

### 3.2 Results of Static Weight Testing

Figure 3-2 shows the data output of the feasibility hardware with no weight added, then with an additional weight of 1.63 lbs added. Since the weight of the seeker assembly itself contributes to the total force measured, the effect of the added weight is the delta between the weight measurements. A weight of 1.80 lbs was measured, and was within 0.17 lbs of the actual additional weight. The overall measurement accuracy is approximately 1% for static weight measurements ( $\frac{.17 \text{ lb}}{16.77 \text{ lb}} \times 100$ ).

The static force measurements were made with the nitrogen feed tube attached. Another static weight measurement was taken with this tube removed, providing a better accuracy of 0.01 lbs out of the 1.63 actual mass weight.

Figure 3-3 shows the resulting force from the firing thruster with a duty cycle of 50 msec on, 10 msec off. The thruster was being driven with nitrogen gas at 2,000 psi pressure.

The total force of the thruster varied from 2 to 2.3 lbs. The bumpiness seen on the waveforms could be caused from several factors, including:

- Line pressure variations: a pressure gauge attached to the feed line showed 200 lb pressure fluctuations during thruster firing.
- Feed line expansion/contraction: the terminal feed line was flexible, braided metal that got noticeably more stiff when it was pressurized.
- Feed line structural feedback: the firing of the thruster created an expected motion component onto the suspended seeker assembly. This motion caused the line to vibrate, providing the possibility of parasitic structural vibrations to be transmitted back to the seeker and sensed by the proximity sensors.
- Inaccuracies in the computation of seeker acceleration. Two methods of acceleration measurement were tried. The first used an accelerometer to sense the accelerations directly. Unfortunately, the "pinging" caused by the opening and closing of the thruster solenoid excited a 5 kHz structural mode in the accelerometer, setting up an electronic ringing component that buried the real thruster-induced accelerations. The second method used the proximity sensor data to derive the acceleration through double differentiation of the motion curve. Due to the coarseness of proximity sensor resolution (0.0002 inch sensitivity) and the 12 bit truncation, this signal had to be heavily filtered to provide reasonable data. Due to this, the acceleration was updated once every 1.0 msec rather than the 0.1 msec data acquisition rate. This filtering could have potentially removed some data, causing additional noise contributions.

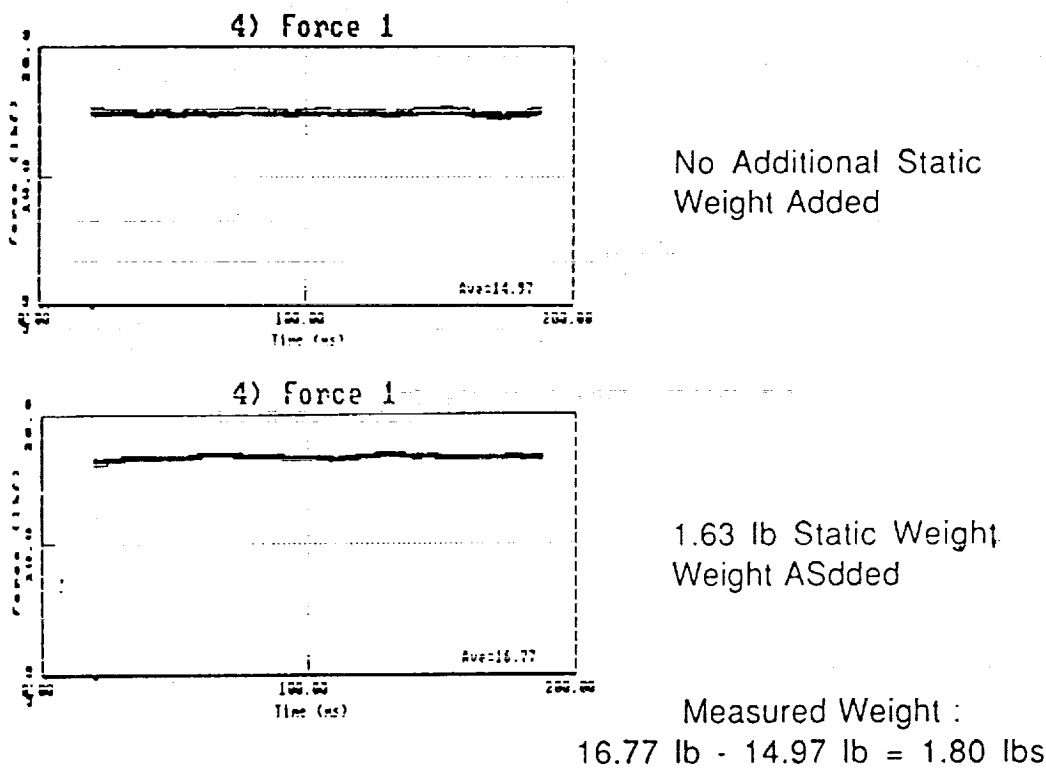


**FIGURE 3-2: FEASIBILITY DATA OUTPUT, STATIC TESTING**

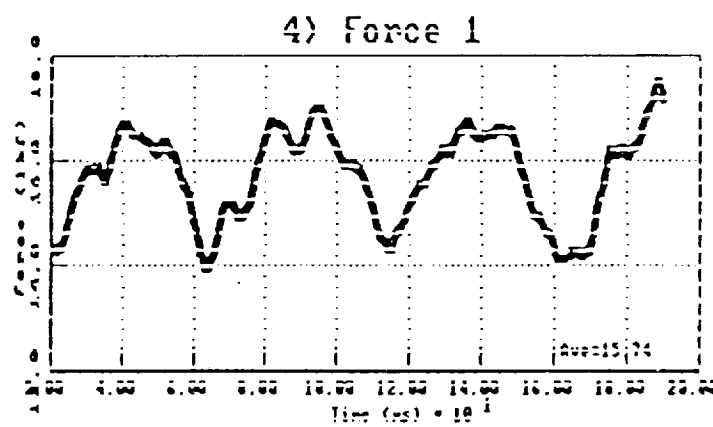


**FIGURE 3-3: FEASIBILITY DATA OUTPUT,  
DYNAMIC THRUSTER TESTING**

A major benefit of the MTTS system is its ability to measure events that occur at frequencies above the magnetic suspension's servo bandwidth. This capability was demonstrated on the feasibility hardware. A 1 kHz motion was induced electronically by injecting an open loop disturbance into the closed loop servo. The data in Figure 3-4 was acquired, tracking the 1 kHz disturbance induced into the seeker mechanical assembly.

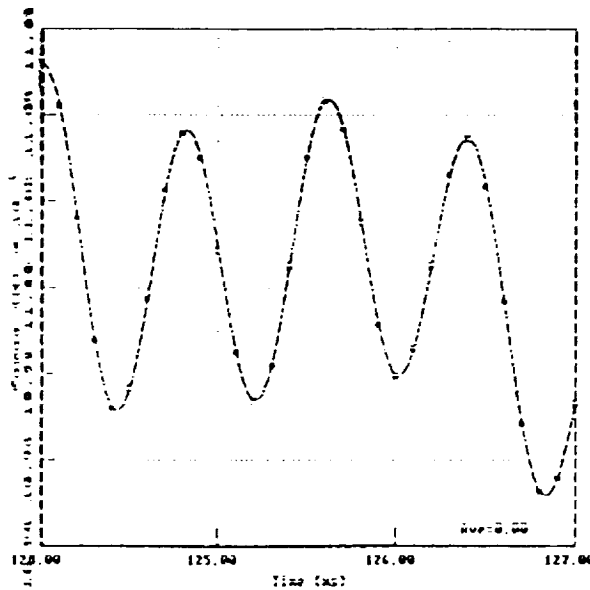


**FIGURE 3-4: MECHANICAL JITTER DATA RESULTS**

## **4.0 FORCE AND TORQUE MESAUREMENT RESOLUTION ANALYSIS**

The force and torque measurement resolution is dependent on the system's ability to accurately measure electromagnet force, gap displacement and acceleration. The analysis that ties the subsystem hardware performance with these parameters follows.

### **4.1 System Resolution Analysis**

Due to the non-linear nature of the system, a computer analysis was required to determine the overall force measurement resolution of the MTTS. The computer analysis modeled the reaction of the MTTS to user-specified thrust levels (see figure 4-1 for an example of a 222.5 Newton thrust force--the force one pole will see during a 100 lb thruster firing). This thrust level was then used to determine the force reaction to the coil (see figure 4-2). Subtracting the coil force from the thruster force yields the resultant force applied to the suspension shaft, on which the thruster resides (see figure 4-3). The shaft velocity and position change is then determined from the resultant force (see figures 4-4 and 4-5). The actual coil current can also be determined from the coil force curve (see figure 4-6).

Figures 4-1 through 4-6 show how the actual system parameters are determined from a thrust event. By using the position curve to emulate proximity sensor data, the coil current curve to emulate current measurement data, and shaft acceleration data to emulate the acceleration, the thruster force can be computed in the same way as it would be by the MTTS's data acquisition system. The thruster force is then re-computed with coil current measuring resolution, proximity sensor resolution and accelerometer resolution taken into account. These two results are used to determine the RMS error starting at 100 micro-seconds after thrust initiation, and ending 8 milliseconds into the thrust.

### **4.2 Analysis Results of Linear Thrust Case**

Overall linear force errors were computed for 2 thrust levels: 2.5 lbs and 100 lbs. The results are given in figures 4-7 and 4-8, and in Table 4-1. In both cases, the total weight of the suspended object (vehicle plus associated fixture supports) was estimated to be 20 lbs. The resulting total RMS error combines the accumulated errors in two poles needed to obtain the total thruster force in a particular direction.

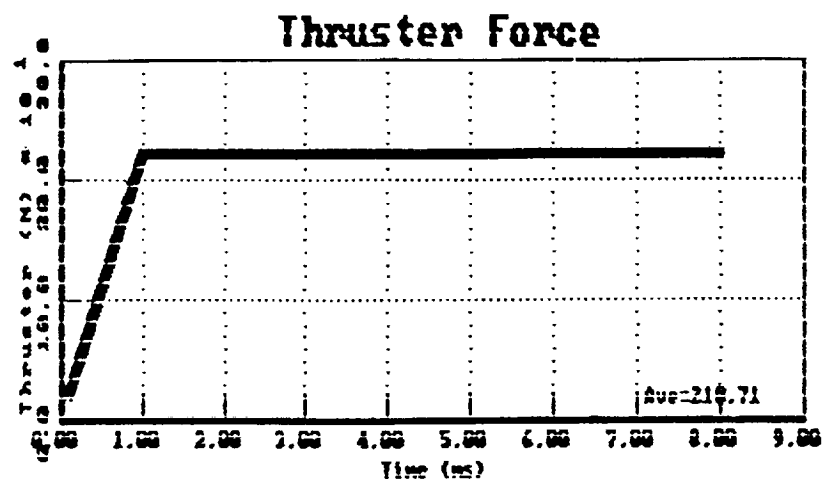


Figure 4-1: 100 lb Thruster Force On a Single Pole

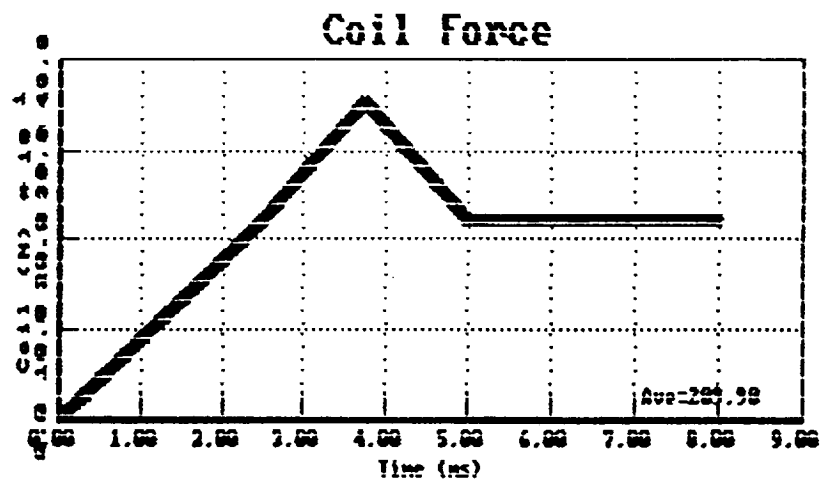


Figure 4-2: Resulting Coil Force from 100 lb Thrust

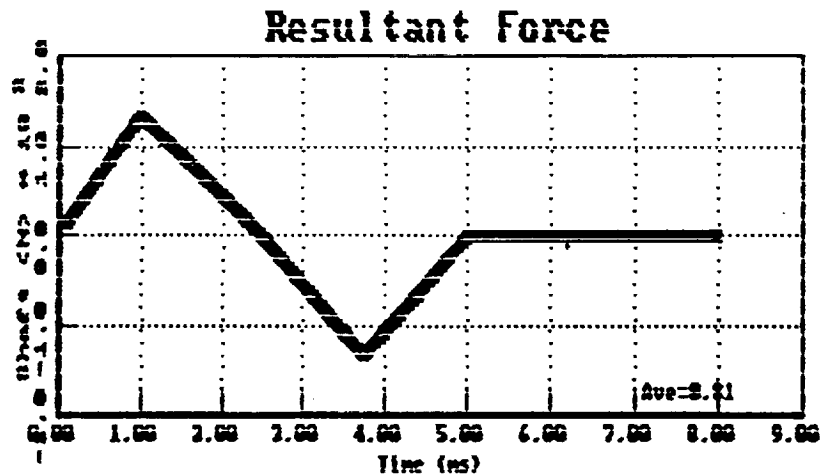


Figure 4-3: Resultant Shaft Force  
(Thruster Force Minus Coil Force)

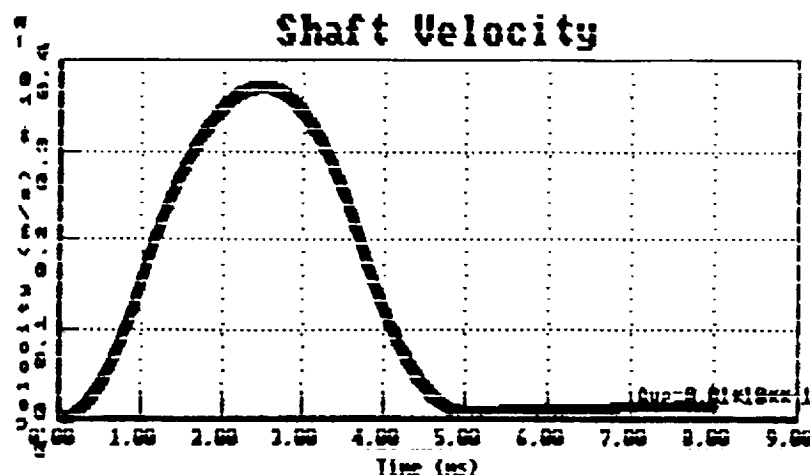


Figure 4-4: Shaft Velocity Due to Resultant Force

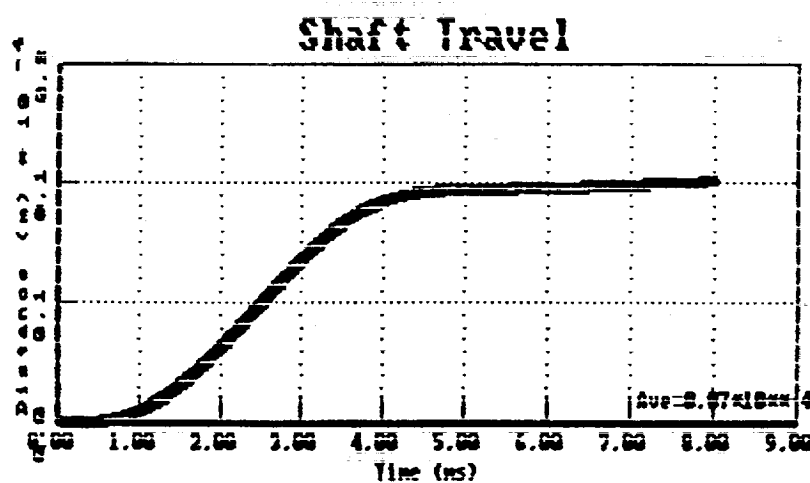


Figure 4-5: Shaft Travel Due to Resultant Force

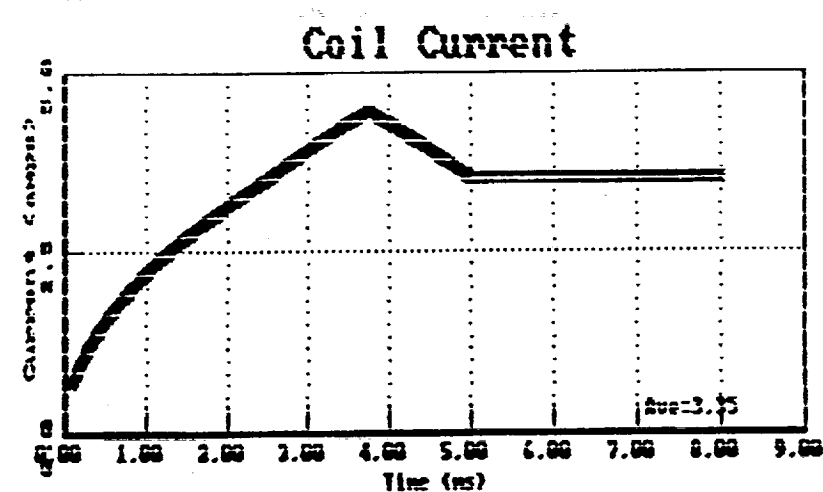


Figure 4-6: Coil Current

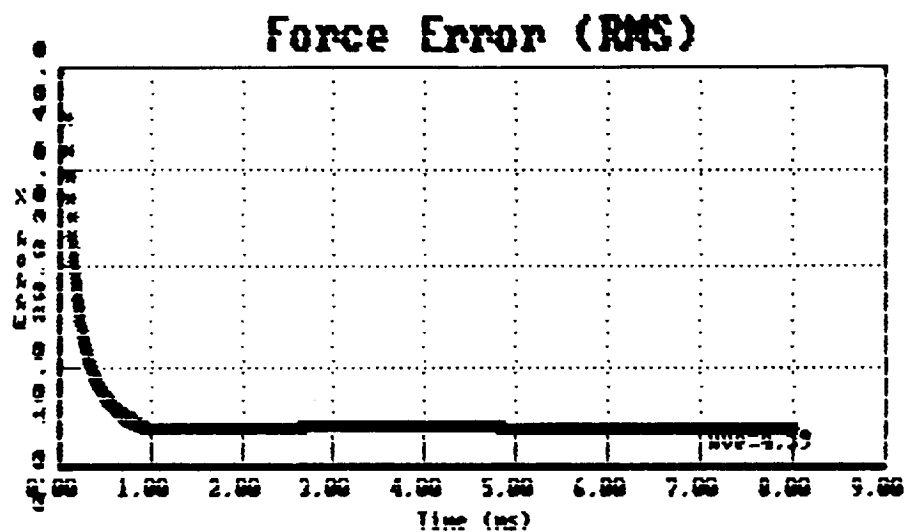


Figure 4-7: Total RMS Force Error for 2.5 lb Thruster

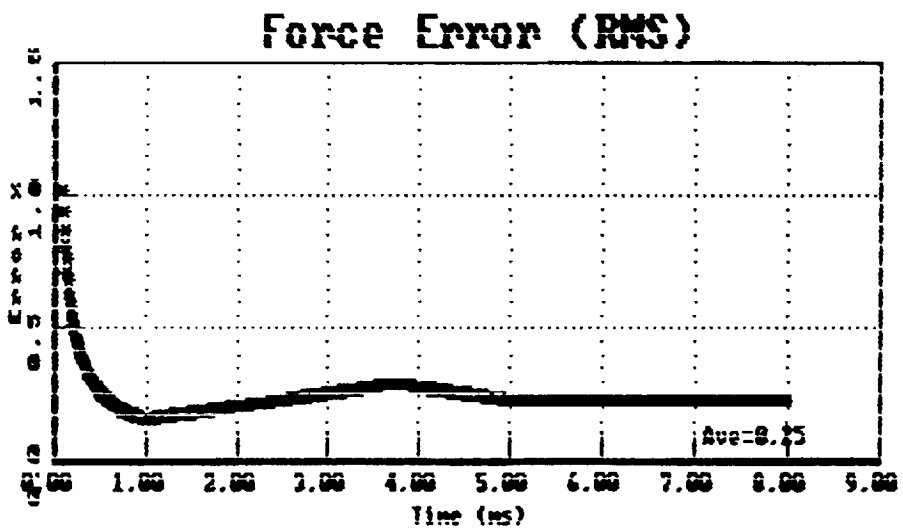


Figure 4-8: Total RMS Force Error for 100 lb Thruster

TABLE 4-1: PERCENT TOTAL FORCE ERROR Vs. TIME

Time (MSec)	Percent Error*	
	2.5 lbs	100 lbs
0.1	34.9	1.03
0.2	17.7	.56
0.3	11.9	.40
0.4	9.0	.32
0.5	7.3	.27
0.6	6.1	.23
0.7	5.3	.21
0.8	4.6	.19
0.9	4.1	.18
1.0	3.7	.16
2.0	3.9	.21
3.0	4.0	.26
4.0	4.1	.29
5.0	4.0	.24
6.0	4.0	.24
7.0	4.0	.24
8.0	4.0	.24

\* Current Measurement Resolution = 0.0005 Amps  
Proximity Sensor Resolution =  $1.27 \times 10^{-7}$  Meters  
Accelerometer Resolution =  $3.0 \times 10^{-4}$  G's

The torque measurement resolution is a function of the force resolution computed above, plus the physical distance between the two radial magnetic bearings and the various moments of inertia. These parameters will be determined during the design phase. Once the distance and moments of inertia are available, an analysis providing the torque measurement resolution of the MTTS will be performed.